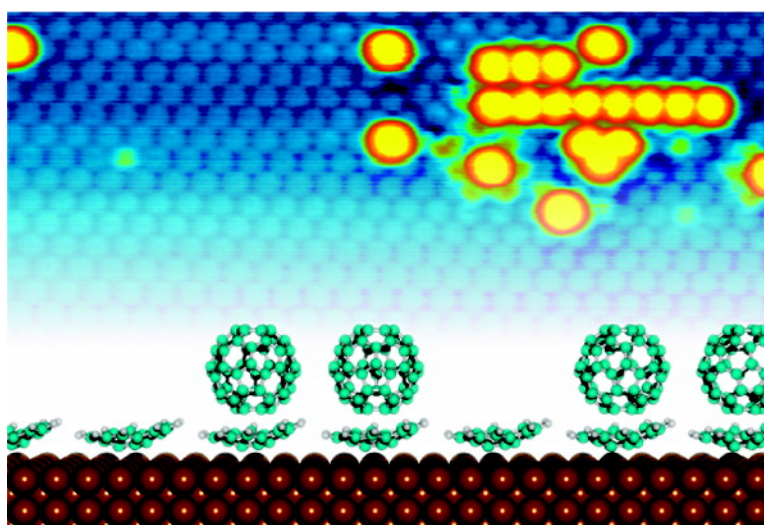


C/Corannulene on Cu(110): A Surface-Supported Bistable Buckybowl–Buckyball Host–Guest System

Wende Xiao, Daniele Passerone, Pascal Ruffieux, Kamel AtMansour, Oliver Grning, Erio Tosatti, Jay S. Siegel, and Roman Fasel

J. Am. Chem. Soc., **2008**, 130 (14), 4767-4771 • DOI: 10.1021/ja077816l

Downloaded from <http://pubs.acs.org> on February 8, 2009



More About This Article

Additional resources and features associated with this article are available within the HTML version:

- Supporting Information
- Links to the 2 articles that cite this article, as of the time of this article download
- Access to high resolution figures
- Links to articles and content related to this article
- Copyright permission to reproduce figures and/or text from this article

[View the Full Text HTML](#)

C₆₀/Corannulene on Cu(110): A Surface-Supported Bistable Buckybowl–Buckyball Host–Guest System

Wende Xiao,[†] Daniele Passerone,[†] Pascal Ruffieux,[†] Kamel Ait–Mansour,[†]
Oliver Gröning,[†] Erio Tosatti,[‡] Jay S. Siegel,[§] and Roman Fasel^{*,†}

nanotech@surfaces Laboratory, Empa, Swiss Federal Laboratories for Materials Testing and Research, Feuerwerkerstrasse 39, 3602 Thun, Switzerland, and Ueberlandstrasse 129, 8600 Dübendorf, Switzerland, International School for Advanced Studies, INFN/CNR/DEMOCRITOS, and International Centre for Theoretical Physics, 34014 Trieste, Italy, and Department of Organic Chemistry, University of Zurich, Winterthurerstr. 190, 8057 Zurich, Switzerland

Received October 11, 2007; E-mail: roman.fasel@empa.ch

Abstract: Corannulene (COR) buckybowls were proposed as near ideal hosts for fullerene C₆₀, but direct complexation of C₆₀ and COR has remained a challenge in supramolecular chemistry. We report the formation of surface-supported COR–C₆₀ host–guest complexes by deposition of C₆₀ onto a COR lattice on Cu(110). Variable-temperature scanning tunneling microscopy studies reveal two distinctly different states of C₆₀ on the COR host lattice, with different binding energies and bowl–ball separations. The transition from a weakly bound precursor state to a strongly bound host–guest complex is found to be thermally activated. Simple model calculations show that this bistability originates from a subtle interplay between homo- and heteromolecular interactions.

Introduction

Molecular hosts that accommodate C₆₀ and/or C₇₀, for example, calix[8]arene,¹ porphyrins,² and cyclothiophene,³ as well as two- or three-dimensional (2D or 3D) supramolecular networks hosting C₆₀ have gained considerable interest due to their importance in materials chemistry.⁴ Corannulene (C₂₀H₁₀, COR),⁵ the simplest bowl-shaped fullerene fragment, offers a natural structural advantage as a host for C₆₀. For optimum “face-to-face” contact, the host should have a complementary structure to the convex surface of C₆₀, as is the case for the concave surface of COR. Moreover, the lower skeletal curvature of COR renders it electron rich compared with fullerene and deeper fragments,⁶ which is anticipated to augment the binding to C₆₀. COR forms a stable complex with (C₆₀)⁺ in the gas

phase,⁷ and COR derivatives bearing electron-rich arms complex neutral C₆₀ in solution.^{8,9} Recently, a molecular cleft comprising two COR fragments provided evidence for neutral buckyball–buckybowl complexation through convex–concave “ball-and-socket” π – π interactions.¹⁰

Here, we report the formation of a surface-supported COR–C₆₀ host–guest system on Cu(110) in ultrahigh vacuum (UHV). On Cu(110), the COR bowl openings point away from the surface, and a close-packed monolayer of COR thus represents a highly regular host lattice.¹¹ In situ variable-temperature scanning tunneling microscopy (VT-STM) studies reveal two distinctly different states of C₆₀ on the COR host lattice, with different binding energies and bowl–ball separations. The transition from a weakly bound precursor state to a strongly bound host–guest complex is found to be thermally activated. This bistability originates from a subtle interplay between homo- and heteromolecular interactions.

Experimental Section

Experiments were carried out in a commercial UHV VT-STM system (Omicron Nanotechnology GmbH) equipped with low-energy electron diffraction (LEED) and standard surface preparation facilities. The Cu(110) single crystal (Surface Preparation Laboratories) was prepared

[†] Swiss Federal Laboratories for Materials Testing and Research.

[‡] INFN/CNR/DEMOCRITOS.

[§] University of Zurich.

- (1) Pan, G.; Liu, J.; Zhang, H.; Wan, L.; Zheng, Q.; Bai, C. *Angew. Chem., Int. Ed.* **2003**, *42*, 2747.
- (2) (a) Bonifazi, D.; Spillmann, H.; Kiebele, A.; de Wild, M.; Seiler, P.; Cheng, F.; Güntherodt, H.; Jung, T.; Diederich, F. *Angew. Chem., Int. Ed.* **2004**, *43*, 4759. (b) Yoshimoto, S.; Tsutsumi, E.; Honda, Y.; Murata, Y.; Murata, M.; Komatsu, K.; Ito, O.; Itaya, K. *Angew. Chem., Int. Ed.* **2004**, *43*, 3044. (c) Boyd, P. D. W.; Reed, C. A. *Acc. Chem. Res.* **2005**, *38*, 235.
- (3) Mena-Osteritz, E.; Bäuerle, P. *Adv. Mater.* **2006**, *18*, 447.
- (4) (a) Theobald, J. A.; Oxtoby, N. S.; Phillips, M. A.; Champness, N. R.; Beton, P. H. *Nature* **2003**, *424*, 1029. (b) Wang, Z.; Dötz, F.; Enkelmann, V.; Müllen, K. *Angew. Chem.* **2005**, *117*, 1273. (c) Stepanow, S.; Lingenfelder, M.; Dmitriev, A.; Spillmann, H.; Delvigne, E.; Lin, N.; Deng, X.; Cai, C.; Barth, J. V.; Kern, K. *Nat. Mater.* **2004**, *3*, 229. (d) Pérez, E. M.; Sierra, M.; Sánchez, L.; Torres, M. R.; Viruela, R.; Viruela, P. M.; Ortí, E.; Martín, N. *Angew. Chem., Int. Ed.* **2007**, *46*, 1847.
- (5) (a) Barth, W. E.; Lawton, R. G. *J. Am. Chem. Soc.* **1966**, *88*, 380. (b) Wu, Y.-T.; Siegel, J. S. *Chem. Rev.* **2006**, *106*, 4843.
- (6) (a) Baldrige, K. K.; Siegel, J. S. *Theor. Chem. Acta* **1997**, *97*, 67. (b) Seiders, T. J.; Gleiter, R.; Baldrige, K. K.; Siegel, J. S. *Tetrahedron Lett.* **2000**, 4519.

- (7) Becker, H.; Javahery, G.; Petrie, S.; Cheng, P.; Schwarz, H.; Scott, L. T.; Bohme, D. K. *J. Am. Chem. Soc.* **1993**, *115*, 11636.
- (8) Mizyed, S.; Georghiou, P. E.; Bancu, M.; Cuadra, B.; Rai, A. K.; Cheng, P.; Scott, L. T. *J. Am. Chem. Soc.* **2001**, *123*, 12770.
- (9) Georghiou, P. E.; Tran, A. H.; Mizyed, S.; Bancu, M.; Scott, L. T. *J. Org. Chem.* **2005**, *70*, 6158.
- (10) Sygula, A.; Fronczek, F. R.; Sygula, R.; Rabideau, P. W.; Olmstead, M. M. *J. Am. Chem. Soc.* **2007**, *129*, 3842.
- (11) Parschau, M.; Fasel, R.; Heinz, E.-H.; Gröning, O.; Brandenberger, L.; Schillinger, R.; Greber, Th.; Seitsonen, A. P.; Wu, Y.-P.; Siegel, J. S. *Angew. Chem., Int. Ed.* **2007**, *46*, 8258.

using repeated cycles of sputtering with argon ions (typically at an argon pressure of 2×10^{-5} mbar and an acceleration voltage of 1.5 kV) and annealing to ~ 700 K. Before deposition of COR, cleanliness and surface order were monitored by STM and LEED. COR overlayers were prepared by thermal sublimation from a Knudsen-cell-type evaporator at a temperature of 360 K, while the Cu(110) substrate was heated to 400 K. C_{60} was deposited on COR overlayers from a second Knudsen-cell-type evaporator at a temperature of 670 K with the sample held at low temperature (LT, ~ 100 K), room temperature (RT), or at slightly elevated temperature (ET, 300–400 K). STM images were acquired in constant-current mode at RT (for RT or ET deposits) or after cooling of the sample to 40 K (for LT deposits).

Gas-phase calculations of the COR– C_{60} complex were performed with the GAMESS-US package at the MP-2 level,¹² with the CC-pVDZ basis set and after correction of the basis set superposition error.¹³ Complementary molecular mechanics (MM) calculations were performed with the AMBER99 force field as implemented in the HyperChem, version 7, program.¹⁴ COR and C_{60} conformations as determined from geometry optimizations in vacuum at PM3 level were used for the MM calculations.

Results and Discussion

Vapor deposition of COR onto the Cu(110) surface results in a close-packed monolayer exhibiting enantiomorphous domains (Figure 1a).¹¹ The unit cells of the quasi-hexagonal λ and ρ domains account for three different nearest-neighbor distances of 10.5, 10.8, and 11.1 Å. Intramolecular resolution images such as the one shown in Figure 1b illustrate that the COR bowl openings point away from the surface. Synchrotron-radiation X-ray photoelectron diffraction (XPD) experiments reveal that the C_{5v} molecular axis is inclined away from the surface normal by 6° along the close-packed $\langle 1\bar{1}0 \rangle$ surface direction, toward an adjoining six-membered ring.¹¹ Figure 1c presents the corresponding structural model of the ρ -domain of the COR monolayer on Cu(110) with molecular orientations as reported previously.¹¹ Molecular arrangements of λ and ρ domains are related to each other by mirror symmetry with respect to the $(\bar{1}10)$ plane perpendicular to the surface. Due to the 2-fold rotational symmetry of the Cu(110) surface, both enantiomorphous domains (λ and ρ) furthermore take two equivalent orientations related by a 180° rotation around the surface normal.

In order to explore the ability of this surface-supported lattice of COR bowl openings to accommodate C_{60} guests (Figure 1d), the fullerene C_{60} was evaporated onto the buckybowl array at different substrate temperatures. For 0.15 monolayer (ML) of C_{60} deposited onto the host lattice held at RT or ET, we observe individual C_{60} molecules on top of the COR lattice, as well as small C_{60} aggregates accumulated at domain boundaries and step edges (Figure 2a), suggesting a high mobility of C_{60} on the COR lattice before its stabilization. Although the C_{60} aggregates are not close-packed, they indicate a net attractive or cohesive intermolecular interaction between C_{60} molecules. A detailed analysis of close-up STM images such as the one shown in Figure 2b reveals that each C_{60} guest is located directly above a COR host. The C_{60} guests appear as featureless spherical

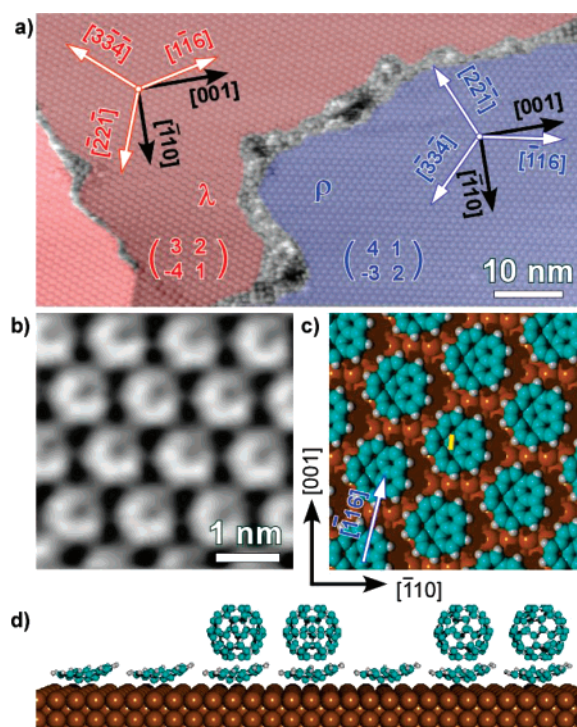


Figure 1. The COR host lattice: (a) STM image of a COR monolayer on Cu(110) revealing enantiomorphous λ - and ρ -domains. High-symmetry directions of the Cu(110) surface (black arrows) and the close-packed directions of the COR lattice (white arrows) are indicated. (b) High-resolution STM image revealing the bowl shape of COR. (c) Structural model of the ρ -domain with molecular orientations as determined from XPD experiments.¹¹ A 6° tilt of the C_{5v} axis along the $[1\bar{1}0]$ direction causes a C–C bond between a C6 and the C5 ring (highlighted in yellow) being closest to the surface. (d) Schematic illustration of the surface-supported COR host lattice, with some of the host sites occupied by fullerene C_{60} guests.

protrusions in high-resolution STM images acquired at RT, in contrast to the ones located at defect sites which show intramolecular features (see Figure S1 of the Supporting Information), suggesting a quasi-free rotation of the C_{60} ball within the COR bowl. Such rotation is not unexpected given the minor differences in binding energy (~ 0.02 eV) between different relative COR– C_{60} cage orientations.¹⁵ The apparent height of C_{60} measured with respect to the COR layer is 4.5 ± 0.2 Å (see parts b and f of Figure 2), similar to that of C_{60} adsorbed on a porphyrin monolayer at RT.^{2a} Figure 2c shows a schematic representation of the corresponding COR– C_{60} host–guest complex on Cu(110).

To verify that the C_{60} molecules are indeed located directly above a COR bowl and not simply embedded within the COR overlayer, we separately deposited COR and C_{60} on the clean Cu(110) surface. The apparent heights of COR and C_{60} both sitting directly on Cu(110) are measured to be 1.1 ± 0.2 Å and 4.5 ± 0.2 Å, respectively, with respect to the bare substrate surface. Assuming that each C_{60} replaces a COR and binds to the Cu(110) surface after C_{60} deposition on the COR lattice, the apparent height of C_{60} with respect to the COR layer is thus expected to be about 3.4 Å, much lower than the measured value of 4.5 Å. For further confirmation of the proposed host–guest structural model, we performed repositioning of C_{60} with the STM tip. Most of our attempts failed even with tunneling

(12) Schmidt, M. W.; Baldrige, K. K.; Boatz, J. A.; Elbert, S. T.; Gordon, M. S.; Jensen, J. H.; Kosecki, S.; Matsunaga, N.; Nguyen, K. A.; Su, S. J.; Windus, T. L.; Dupuis, M.; Montgomery, J. A. *J. Comput. Chem.* **1993**, *14*, 134.

(13) Boys, S. F.; Bernardi, F. *Mol. Phys.* **1970**, *19*, 558.

(14) HyperChem, release 7.0; Hypercube, Inc.: Gainesville, FL 32601. <http://www.hyper.com/>.

(15) Binding energies were calculated with the AMBER99 force field for different C_{60} orientations and vertical positions above the COR bowl.

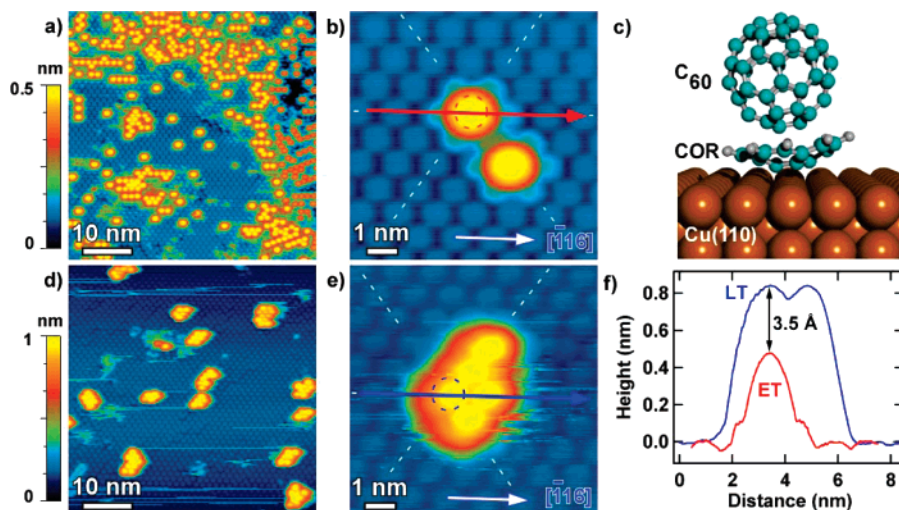


Figure 2. (a) Topographic STM image taken after the deposition of ~ 0.15 ML C_{60} on the COR lattice at ET. (b) Individual C_{60} molecules adsorbed on top of underlying COR bowls at ET. (c) Schematic representation of an individual COR– C_{60} host–guest complex on Cu(110). (d) STM image showing random distribution of small close-packed C_{60} clusters on the COR lattice after LT deposition of ~ 0.05 ML C_{60} . (e) Close-up of a C_{60} cluster on the COR lattice at LT. (f) Line profiles across C_{60} molecules deposited at ET and at LT, as indicated in b and e.

conditions that lead to a disordering of the underlying COR lattice. On the other hand, we occasionally succeeded in manipulating C_{60} molecules away from their original positions by an abrupt reduction of the gap voltage during scanning (See Figure S2 of the Supporting Information). We found that C_{60} molecules have identical apparent height with respect to the tip-created C_{60} vacancies and to the original ones (empty COR hosts), confirming that C_{60} is indeed located above a COR bowl. The difficulty of C_{60} relocation furthermore indicates the formation of a strongly bound COR– C_{60} host–guest complex.

We have investigated the chemical binding of the COR– C_{60} host–guest complex by means of RT ultraviolet photoelectron spectroscopy experiments and ab initio calculations at the MP2 level. Comparison of valence band spectra of the surface-supported COR– C_{60} host–guest complexes, clean Cu(110), C_{60} on Cu(110), and the empty COR host lattice on Cu(110) (see Figure S3 of the Supporting Information) reveals the absence of significant charge transfer to the fullerene molecules. Calculations for a gas-phase COR– C_{60} pair give a binding energy of 1.1 eV in the (nonoptimal) geometry of two pentagons facing each other, with an equilibrium distance between the bottom of COR and the lower pentagon of C_{60} of 3.3 ± 0.1 Å, and no evidence for charge transfer between the two molecules (see the Supporting Information). We thus conclude that the COR– C_{60} host–guest binding is mainly due to π – π interaction between the almost perfectly complementary convex and concave faces of C_{60} and COR, with possibly a further (albeit weaker) contribution resulting from CH– π interaction between the rim of COR and C_{60} .

Interestingly, the aggregates of COR– C_{60} host–guest complexes shown in Figure 2a are not 2D close-packed, unlike islands of C_{60} directly grown on the Cu(110) surface.¹⁶ Instead, linear chains along two preferential directions (Figure 3a) are observed. Although each COR domain has three close-packed directions, C_{60} chains form only along one of them. Close-up

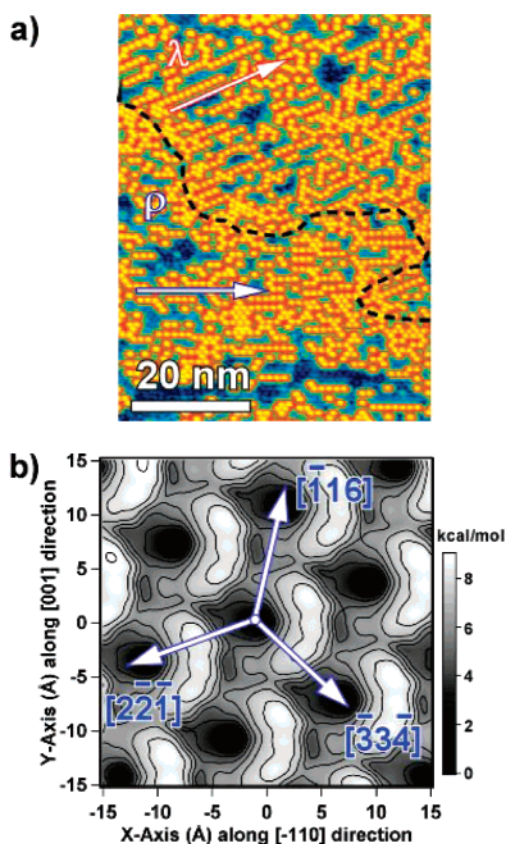


Figure 3. (a) Topography after deposition of ~ 0.4 ML C_{60} on the COR lattice held at ET, showing the formation of C_{60} –COR host–guest complexes along two preferential directions indicated by arrows. A boundary between COR λ - and ρ -domains is indicated by a dashed line. (b) Calculated energy landscape for C_{60} diffusion on a ρ -domain of the COR lattice. The diffusion barrier is lowest along the $[1\bar{1}6]$ direction. The corresponding geometry of the COR cluster used for the calculations is shown in Figure 1c.

STM images reveal that the direction of linear chains relates to the chirality of the COR domain: $[\bar{1}\bar{1}6]$ for λ domains, and $[\bar{1}\bar{1}6]$ for ρ domains. The 6° tilt of the C_{5v} axis of COR away from the Cu(110) surface normal leads to an inhomogeneous lattice,¹¹ with “grooves” along the $[\bar{1}\bar{1}6]$ and $[\bar{1}\bar{1}6]$ directions

(16) (a) Pedersen, M. Ø.; Murray, P. W.; Lægsgaard, E.; Stensgaard, I.; Besenbacher, F. *Surf. Sci.* **1997**, *389*, 300. (b) Murray, P. W.; Pedersen, M. Ø.; Lægsgaard, E.; Stensgaard, I.; Besenbacher, F. *Phys. Rev. B: Condens. Matter Mater. Phys.* **1997**, *55*, 9360. (c) Fasel, R.; Agostino, R. G.; Aebi, P.; Schlapbach, L. *Phys. Rev. B: Condens. Matter Mater. Phys.* **1999**, *60*, 4517.

in the λ - and ρ -domains, respectively (see Figure 1c). It is thus anticipated that these grooves provide a lower energy barrier for C_{60} diffusion than the other close-packed directions, where the C_{60} has to “climb up” from the groove across the potential well of the protruding edge of COR. The calculated energy landscape (Figure 3b) for C_{60} diffusion on the ρ -domain of COR confirms this picture:¹⁷ The path along the groove ($[1\bar{1}6]$ direction) has the lowest diffusion barrier, which is, then, the preferential direction for the formation of C_{60} linear chains. We note that this mechanism is very different from the one reported for the formation of C_{60} linear chains on a porphyrin monolayer via C_{60} -induced conformational changes of the underlying porphyrin layer.^{2a}

A totally different situation is encountered after deposition of C_{60} onto the COR host lattice with the substrate kept at LT. In contrast to deposition at ET, LT C_{60} deposition results in small close-packed 2D clusters including several molecules (as the one displayed in Figure 2e) even at a coverage of only ~ 0.05 ML. These clusters are randomly distributed on the COR lattice, as seen in Figure 2d. Not surprisingly, the C_{60} molecules take on almost the same (careful analysis reveals a difference within a few percent, as described below) lateral adsorption site as they do when deposited at ET: They are exclusively located on top of underlying COR bowls (Figure 2e). However, line profiles (Figure 2f) reveal dramatically different apparent heights of C_{60} with respect to the COR layer for LT and ET deposits (7.8 ± 0.5 Å and 4.5 ± 0.2 Å, respectively). Due to the importance of electronic effects and tunneling matrix elements,¹⁸ this apparent height difference can only qualitatively be related to an increase in C_{60} –COR separation distance. Nevertheless, it strongly suggests two significantly different states for C_{60} on COR. Although C_{60} is found directly on top of an underlying COR bowl, the binding between C_{60} and COR is very weak for C_{60} molecules having an apparent height of 7.8 Å with respect to the COR layer at LT. Scanning under “normal” tunneling conditions (typically -2.2 V/0.02 nA) frequently leads to displacement of C_{60} , while the underlying COR lattice remains intact. At RT and above, the C_{60} ball is strongly bound to the COR bowl directly below and has a short intermolecular distance, while the LT C_{60} adsorption state is only weakly bound to the COR bowl, and there is a larger intermolecular distance.

The mechanism that leads to this bistable behavior cannot be understood from ab initio calculations considering a single COR– C_{60} pair only, since apart from the strongly bound host–guest complex discussed above, they yield no second minimum energy configuration at larger ball–bowl distances. In order to understand the LT formation of weakly bound 2D C_{60} clusters on top of the COR lattice, we have to recall that the natural nearest-neighbor distance within a C_{60} layer is $d = 10.05$ Å.¹⁹ Similar situations occurring in surface science have been understood in the framework of the Frenkel–Kontorova (FK) model.²⁰ The FK model, in its original version, describes the equilibrium states of a linear chain of particles with harmonic lateral interactions and a harmonic external potential with different

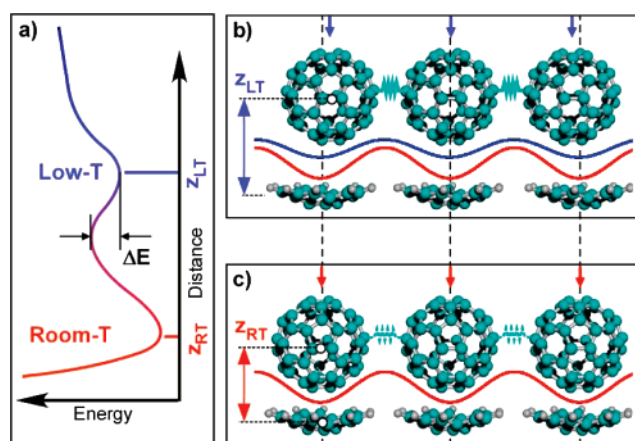


Figure 4. Schematic one-dimensional model of the bistable behavior for a C_{60} island on a nonperfectly matched COR substrate. There is competition between a state where all C_{60} guests lie close to the surface in the well of the COR hosts (c) and a state where the C_{60} profit of the lateral interaction but have to “pay” for the nonperfect matching with the substrate (b). The minimum energy path between these two states shows an energy barrier (a).

periodicity. We adapted this idea to our case (Figure 4): a C_{60} island is a finite overlayer, and the external potential is given by the interaction of the island with the underlying COR lattice. For numerical simulations (see the Supporting Information), we chose the model substrate potential (COR– C_{60} interaction) to be very selective with respect to the lateral position and selected the Girifalco potential for the C_{60} – C_{60} interaction.²¹ This results in a strongly anharmonic corrugation, which favors the emergence of two different classes of solutions when the island size is larger than a critical value. The first class of solutions shows C_{60} islands floating above the COR lattice with a C_{60} – C_{60} spacing close to 10.05 Å (Figure 4b), whereas the other class of solutions predicts the fullerenes to stay closer to the surface and to adapt to the substrate potential given by the COR lattice (Figure 4c). The two solutions are separated by an energy barrier, in agreement with experiment. Already these simple model calculations thus show how the collective effect of the cohesive energy within a C_{60} island creates a barrier to COR– C_{60} host–guest complex formation: Due to the lattice mismatch, at LT the advantage of the cohesive energy overcomes the nonideal matching with the substrate, and 2D C_{60} islands with short intermolecular distances are formed at a height above the COR lattice where the corrugation is small (see Figure 4).

This picture is experimentally supported by different observations. First, a careful analysis of STM images of LT C_{60} islands reveals an imperfect matching with the substrate: Along the $[1\bar{1}6]$ and $[1\bar{1}\bar{6}]$ directions of the ρ - and λ -domains, respectively, C_{60} – C_{60} distances were measured to be 10.5 ± 0.2 Å. This is significantly smaller than the 11.1 Å periodicity of the underlying COR lattice along this direction.²² Second, we note that the LT C_{60} clusters exhibit a preferential elongation along the $[3\bar{3}4]$ and $[3\bar{3}\bar{4}]$ directions, which correspond to the shortest COR–COR distance of 10.5 Å (Figure 2d). It is along this direction that the lattice mismatch is smallest and thus the corresponding energy penalty is lowest.

Finally, the behavior of the LT C_{60} clusters upon annealing to RT also conforms to the picture outlined above: The random

(17) Calculations were performed with the AMBER99 force field, for C_{60} at different lateral and vertical positions above the COR host lattice. A COR cluster including 19 molecules with molecular orientations as determined from XPD was used to model the ρ -domain, as shown in Figure 1c.

(18) Hofer, W. A.; *Prog. Surf. Sci.* **2003**, *71*, 147.

(19) Nakamura, J.; Nakayama, T.; Watanabe, S.; Aono, M. *Phys. Rev. Lett.* **2001**, *87*, 48301.

(20) Frenkel, Y.; Kontorova, T. *Phys. Z. Sowjetunion* **1938**, *13*, 1.

(21) Girifalco, L. A. *J. Phys. Chem.* **1991**, *95*, 5370.

(22) A commensurate distance of 11.3 ± 0.3 Å is measured for neighboring C_{60} in the ET host–guest configuration along the same direction.

distribution of close-packed C_{60} clusters on the COR lattice transforms into linear chains (see Figure S4 of the Supporting Information) of strongly bound COR– C_{60} host–guest complexes. The retention of the random distribution of aggregates and the formation of linear chains along the low diffusion barrier $[1\bar{1}6]$ and $[1\bar{1}\bar{6}]$ directions indicate that the crucial step toward COR– C_{60} host–guest complexation is the dissociation of a C_{60} molecule from a close-packed island. Thus, during warm up, shortly after a C_{60} molecule is freed from an island and before its diffusion becomes efficient, it sinks into a COR bowl close to its original position. Concerning the dissociation of a C_{60} cluster as the one shown in Figure 2e, energetically the most expensive step would be for the bottommost molecule to reduce its coordination from 2 to 0 and get free. From the cohesive energy of a C_{60} monolayer (C_{60} coordination of 6) of ~ 1.31 eV,¹⁹ we thus obtain an estimate for the cluster dissociation barrier of 0.44 eV. This translates into a temperature of 150 ± 20 K,²³ in agreement with experiment, and gives an estimate of the activation energy ΔE (see Figure 4) of the observed COR– C_{60} host–guest complexation.

Conclusions

In summary, we have demonstrated the formation of surface-supported COR– C_{60} host–guest complexes by deposition of buckballs onto a buckybowl lattice on Cu(110). COR– C_{60} host–guest complexation is a thermally activated process: At LT, lateral interactions between C_{60} molecules inhibit C_{60} –COR complexation and stabilize 2D C_{60} islands floating far above

the COR lattice. Upon annealing to RT or above, C_{60} molecules dissociate from the 2D islands, sink into the COR bowls, and form strongly bound COR– C_{60} host–guest complexes. These findings highlight the importance of anisotropic environments at surfaces and the utility of convex–concave π – π interactions in the fabrication of surface-supported supramolecular architectures. Due to their complementary faces, buckybawls and their derivatives are useful components for host–guest complexation with fullerenes.

Acknowledgment. We thank K.-H. Ernst for stimulating discussions and a critical reading of the manuscript. Financial support by the European Commission (RADSAS, NMP3-CT-2004-001561), from the Swiss National Science Foundation (NCCR Nanoscale Science), and from the Italian Ministry (PRIN 2006022847) is gratefully acknowledged. The use of computational resources at the Swiss National Superconducting Centre (CSCS) is gratefully acknowledged.

Supporting Information Available: STM image evidencing quasi-free rotation of the C_{60} guests in the COR host bowls; STM manipulation of C_{60} guests out of their positions within the COR host bowls; ultraviolet photoelectron spectroscopy data; transformation of the low-temperature 2D C_{60} islands into strongly bound COR– C_{60} host–guest complexes upon annealing to room temperature; gas-phase calculations for the COR– C_{60} complex; and Frenkel–Kontorova-type model calculations. This material is available free of charge via the Internet at <http://pubs.acs.org>.

(23) Using the Arrhenius formula with an attempt frequency of 10^{13} s^{-1} and an activation energy of 0.44 eV, rate constants between 10^{-4} and 10^0 s^{-1} translate into temperatures between 130 and 170 K.

JA077816L